International Journal of Fuzzy Logic and Intelligent Systems, vol. 7, no. 2, June 2007 pp. 102-108

Fault Detection and Identification of Induction Motors with Current Signals Based on Dynamic Time Warping

Hyeon Bae, Sungshin Kim, and George Vachtsevanos*

School of Electrical and Computer Engineering, Pusan National University, Busan, Korea
***School of Electrical and Computer Engineering, Georgia Institute of Technology, Atlanta, GA, USA**

Abstract

The issues of preventive and condition-based maintenance, online monitoring, system fault detection, diagnosis, and prognosis are of increasing importance. This study introduces a technique to detect and identify faults in induction motors. Stator currents were measured and stored by time domain. The time domain is not suitable for representing current signals, so wavelet transform is used to convert the signals onto frequency domain. The raw signals can not show the significant feature, therefore difference values are applied. The difference values were transformed by wavelet transform and the features are extracted from the transformed signals. The dynamic time warping method was used to identify the four fault types. This study describes the results of detecting fault using wavelet analysis.

Key words : Induction motor, fault detection and diagnosis, wavelet transform, dynamic time warping

1. Introduction

The most popular way of converting electrical energy to mechanical energy is an induction motor. This motor plays an important role in modern industrial plants. The risk of motor failure can be remarkably reduced if normal service conditions can be arranged in advance. In other words, one may avoid very costly expensive downtime by replacing or repairing motors if warning signs of impending failure can be headed. In recent years, fault diagnosis has become a challenging topic for many electric machine researchers. The major faults of electrical machines such as broken rotor bar, cracked rotor end-rings, static and dynamic air-gap irregularities, dynamic eccentricity, and bearing and gearbox failure can be broadly classified [1]. Among the above faults, bearing fault, broken rotor bar, misalignment, unbalance were detected in this study.

The diagnostic methods to identify the faults listed above may involve several different types of fields of science and technology [1], [2]. Many types of signals have been studied for the fault detection of induction motors. However, each technique has advantages and disadvantages with respect to the various types of faults. Several methods such as electromagnetic field monitoring, temperature measurements, radio frequency (RF) emissions monitoring, noise and vibration monitoring, motor current signature analysis (MCSA) were used to detect faults in induction motors in the traditional researches. Among the methods, MCSA was employed to detect and identify the faults in this study.

Manuscript received Mar. 9, 2007; revised Jun. 12, 2007.
This work was supported by the Second stage of Brain Korea 21 Project in 2007 and 2007 overseas dispatch program of Pusan National University.

For properly analysis of the current signals, the time series signals are required to be transformed to frequency domain. In the past studies, Fourier transform has been broadly applied for the task. Although the Fourier transform is an effective method and widely used in signal processing, the transformed signal may lose some time domain information. The limitation of the Fourier transform in analyzing non-stationary signals leads to the introduction of time-frequency or time scale signal processing tools, assuming the independence of each frequency channel when the original signal is decomposed. Therefore, in this study, wavelet transform was used to decompose the current signals. Wavelet transform is a method for time varying or non-stationary signal analysis, and uses a new description of spectral decomposition via the scaling concept. Wavelet theory provides a unified framework for a number of techniques, which have been developed for various signal processing applications [4-7].

However, the raw current signals were not suitable for fault diagnosis in this study. Because the difference between normal land abnormal signals was not so significant, in this study, the difference signals between a normal signal and each fault signal were applied for feature extraction. The difference values were decomposed by wavelet transform in this study. The difference values contain just specific feature values of the faults, because unexpected values of the signals are removed by the difference calculation. This approach reduces the error caused by normal feature values. And because the small signals are converted by wavelet transform, faults can be detected by just detail coefficients of wavelet decomposition.

In this study, instead of using the classification model for fault identification, a pattern matching method was used such as a dynamic time warping method that has advantages of low computation and the training error is not considered. Figure 1

shows the flowchart that includes template generation and fault identification steps.

In this paper, Section 2 describes the methods that are applied in this study and Section 3 shows the data acquisition and preprocessing stages. Section 4 shows the results of the fault detection and identification.

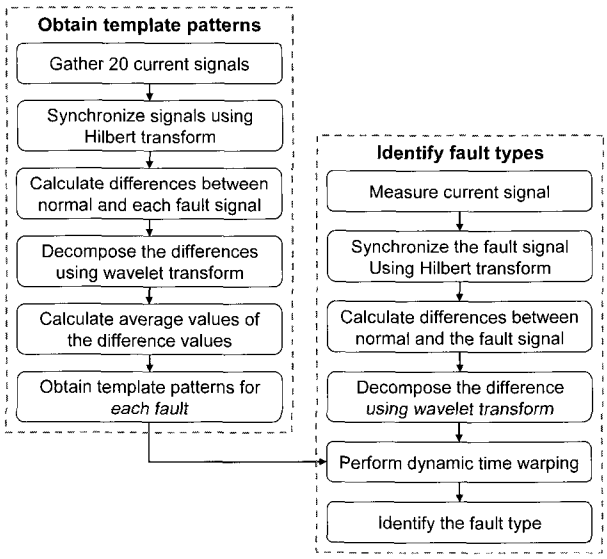

Fig. 1. Flowchart of fault detection and diagnosis.

2. Fault detection and identification methods

2.1 Wavelet transform

Wavelet transform was applied to extract fault features from the difference signals. A wavelet is a function belonging to $L_2(R)$ with a zero average. It is normalized and centered in the in the neighborhood of t=0. A family of time-frequency atoms is obtained by scaling Ψ by a^j and translating is by b [8-10]:

$$\psi_{a,b} = |a|^{\frac{-j}{2}} \psi\left(\frac{t-b}{a^j}\right) \tag{1}$$

These atoms also remain normalized. The wavelet transform of f belonging to $L_2(R)$ at the time b and scale a^j is:

$$Wf(b,a^j) = \left\langle f, \varphi_{b,a^j} \right\rangle = \int_{-\infty}^{\infty} f(t) \frac{1}{\sqrt{a^j}} \varphi^*\left(\frac{t-b}{a^j}\right) dt \tag{2}$$

A real wavelet transform is complete and maintains energy conservation as long as the wavelet satisfies a weak admissibility condition which is:

$$\int_0^{+\infty} \frac{|\Psi(w)|^2}{|w|} dw = \int_{-\infty}^{0} \frac{|\Psi(w)|^2}{|w|} dw = C_\psi < +\infty \tag{3}$$

When $wf(b,a^j)$ is known only for $a<a_0$, to recover f we need a complement of information corresponding to $wf(b,a^j)$ for $a<a_0$.

2.2 Dynamic time warping

Dynamic time warping (DTW) was introduced by Sakoe and Chiba in 1978 [11]. It was used in conjunction with dynamic programming techniques for the recognition of isolated words. DTW has been used in conjunction with a neural network for the recognition of isolated words [12]. In this study, DTW was used to identify the fault type among the four faults.

The DTW algorithm removes timing differences between speech patterns by warping the time axis of one speech pattern until it maximally coincides with the other. All pattern vectors are warped against a reference pattern vector of the same category which has the same number of feature vectors as there are frames in the input layer of the network.

After the relevant feature extraction has taken place, speech patterns can be represented as a sequence of feature vectors,.

$$\begin{aligned} A &= a_1, a_2, \ldots, a_i, \ldots, a_K \\ B &= b_1, b_2, \ldots, b_j, \ldots, b_M \end{aligned} \tag{4}$$

Let A be the reference speech pattern and B be the pattern vector to be aligned against A. Figure 2 shows A and B developed against the i and j axes.

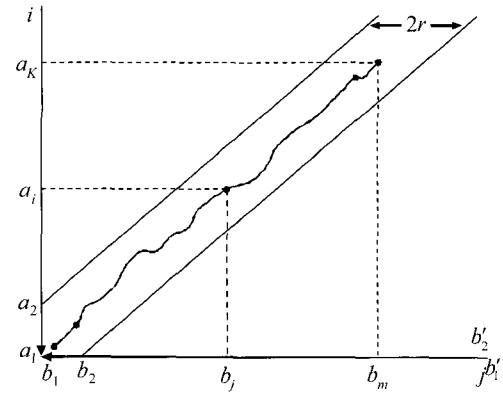

Fig. 2. Warping function and adjustment window.

Consider a warping function F between the input pattern time j and the reference pattern time i, where

$$j = j(i) \tag{5}$$

A measure of the difference between the two feature vectors ai and bj is the distance

$$d(i,j) = \|a_i - b_j\| \tag{6}$$

When the warping function is applied to B this distance becomes

$$d(i, j(i)) = \|a_i - b'_j\| \tag{7}$$

where b'_j is the jth element of B after the warping function has been applied.

The minimum residual distance between A and B is the distance still remaining between them after minimizing the

timing differences between them. The time normalized difference is defined as follows:

$$D(A,B)=\min_{F}\left[\frac{\sum_{i=1}^{K} d(i,j(i))*w(i)}{\sum_{i=1}^{K} w(i)}\right] \quad (8)$$

Applying Dynamic programming principles to the simplified time normalization equation gives the following algorithm for calculating the minimal value of the summation:

The dynamic programming equation is

$$g_i(i,j(i))=\min\left[g_{i-1}(i-1,j(i-1))+d(i,j(i))*w(i)\right] \quad (9)$$

$$D(A,B)=\frac{1}{N} g_K(i(K),j(K)) \quad (10)$$

$$g_1(1,1)=d(1,1)*w(1)=d(1,1) \quad (11)$$

$$g_i(i,j)=d(i,j)+\min\begin{cases} g(i-1,j-1) \\ g(i-1,j-2) \\ g(i-1,j-3) \end{cases} \quad (12)$$

3. Data acquisition and preprocessing

3.1 Test bed for data acquisition

To measure input currents of an induction motor, a current transducer (CT) was used and off-set of the CT and scaling errors of the three-phase currents received from the CT were removed by the low-pass filter (LPF), the 12bit A/D converter, and the D/A converter. The current signals were conditioned and the conditioned signals were collected by the data acquisition board. DC-link capacitors and voltage and current sensors were used and AC circuit breakers were applied to protect the circuit from over current. The main controller was designed for the exclusive controller that consists of a CPU, a memory, an analog signal processor for external interface, gating generator, and a digital in-output board. The model name of the DSP chip is TMS320VC33 that has the high computational speed and can calculate 32bit floating point. Most of the digital logic was developed using EPLD. The main functions of the EPLD include memory decoding, logic circuits for driving the control board, decoder, generating wait signals, generating interrupt signals, calculating motor speed, protecting hardware, and inspecting power devices. The 12bit A/D converter was used to convert analog signals to digital signals and the 12bit high-precision D/A converter was applied to validate input and output variables. The data acquisition device for gathering the current signals can receive 16 channel analog signals maximally and has 16bit resolution. The maximum sampling speed is 200kS/s and the voltage range is ±10V. Figure 3 shows the test bed used in data acquisition and motor control.

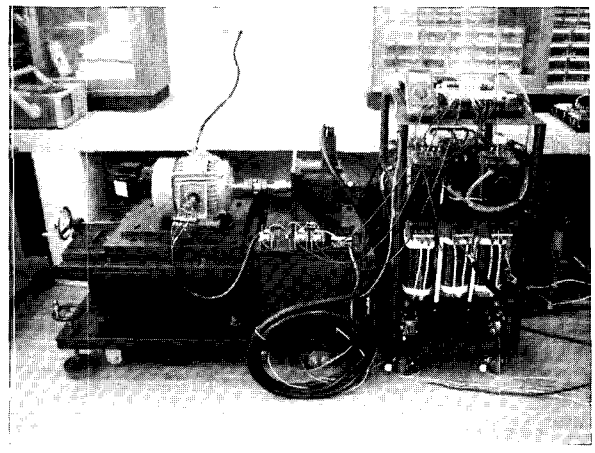

Fig. 3. Test bed for data acquisition.

3.2 Signal measurement and preprocessing

The specification of the measured input current signal under this condition consists of 16,384 sampling numbers, 3kHz maximum frequency, and 2.1333 measuring time. Fault types used in this study are broken rotor, faulty bearing, unbalance, and misalignment. 40 signal sets were measured for each fault. Figure 4 shows the measured signals that show one normal case and one fault case, that is, a broken rotor fault. As shown in the signals, the significant difference does not appear in the raw signals; therefore it is necessary to extract the specific feature from the raw signal for correct diagnosis.

The measured signals were filtered and synchronized for the proper value in fault detection. In this study, the average value divided by one cycle signal was used to reduce the noise of the original signals and Hilbert transform was applied for synch. If the target signals are not synchronized with each other, unexpected results will appear in wavelet decomposition. Hilbert transform is suitable in this study. The well performed preprocessing can guarantee the good performance.

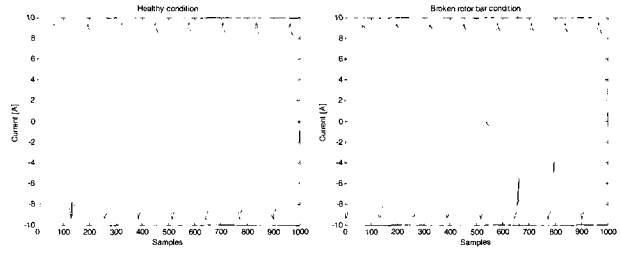

(a) Healthy condition (b) Fault condition

Fig. 4. Synchronized current signals

4. Experimental results

4.1 Feature extraction using difference values

The total signal sets for each fault were 40 and the signals were used for calculating difference values between a normal signal and each fault signal. Therefore, the difference values were 40 for each fault and the difference values were used as features. The difference values were transformed by wavelet

transform and the 1st detail coefficient were gathered for fault identification. 20 signals of 40 signals were averaged to generate templates for the faults. The number of the faults was four, so the number of the templates was also four. The templates prepared were compared with fault signals that include 20 signal sets for each fault. The similarity was calculated by the dynamic time warping method that is one of the template matching methods. If the fault signal is similar with one template, the matching degree can be high and vice verse. Therefore each matching degree for whole fault signals can be calculated by the DTW. Figure 5 shows the diagram and Fig. 6 shows the difference values between a normal signal and fault signals.

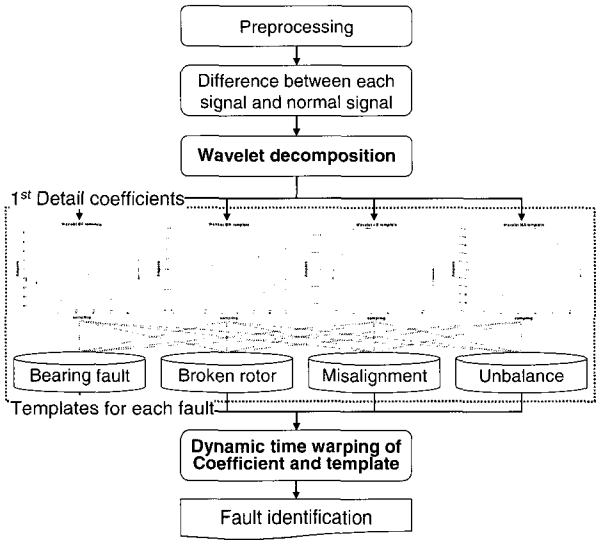

Fig. 5. Feature extraction of the fault features

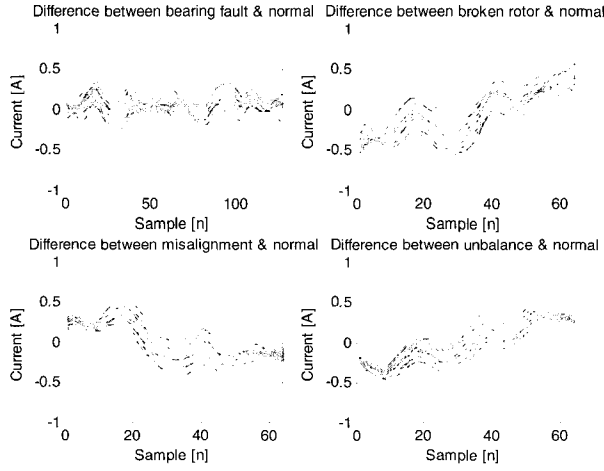

Fig. 6. Difference values of two fault conditions.

4.2 Feature detection using wavelet analysis

In this study, wavelet analysis was used to extract features of the motor faults. Wavelet transform is suitable for time series data mining to extract features of the motor faults because no time information loss happens while transforming. In this study, the 1st detail coefficients of decomposition were treated in detection owing to including information of several faults. Decomposition scales were determined by the trial-and-error method. The Har wavelet function was selected based on experimental experience as providing better performance to perform the decomposition. Figure 7 shows the 1st coefficient for four faults because the 1st coefficient between whole coefficients shows the specific information to detect several types of the faults.

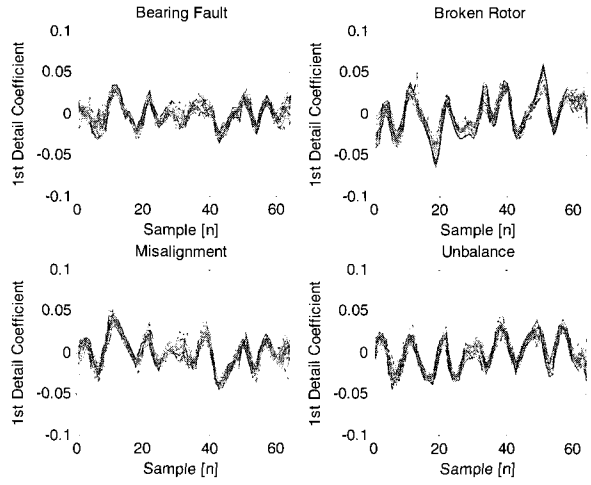

Fig. 7. Detail coefficient of the two fault conditions

4.3 Dynamic time warping

In this study, fault signals were matched with the four templates prepared in advance. The 20 signals sets selected by the hold-out method were used to generate a template for a fault. For fault identification, the rest 20 signal sets of 40 signals were applied. The dynamic time warping method was implemented in fault identification that calculates the matching degree between a template signal and a fault signal. Figure 8 shows the results of time warping and dynamic programming using a matched case with one template signal. Figure 9 shows the results using the unmatched case with one template signal. The matching degree can be evaluated by similarity with a diagonal line. If two sets are similar each other, the test line should be close to the diagonal line.

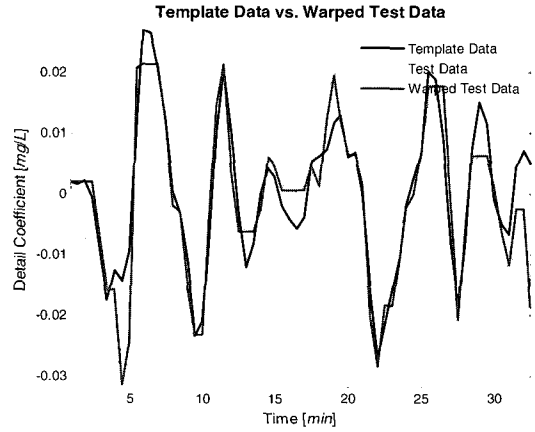

(a) Result of time warping

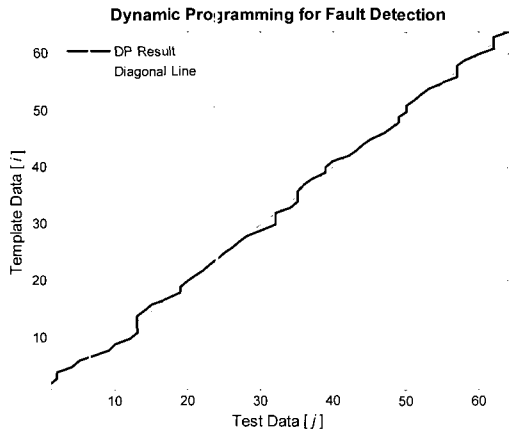

(b) Result of dynamic programming

Fig. 8. DTW result with two similar data sets.

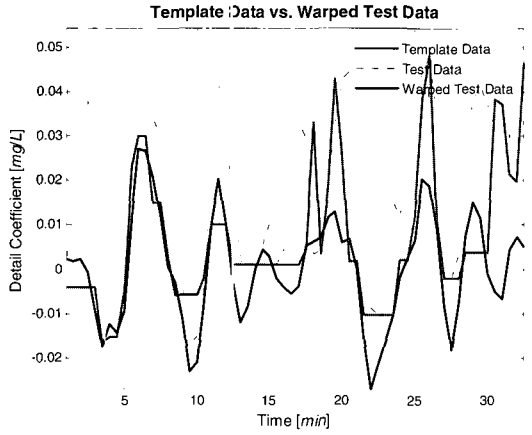

(a) Result of time warping

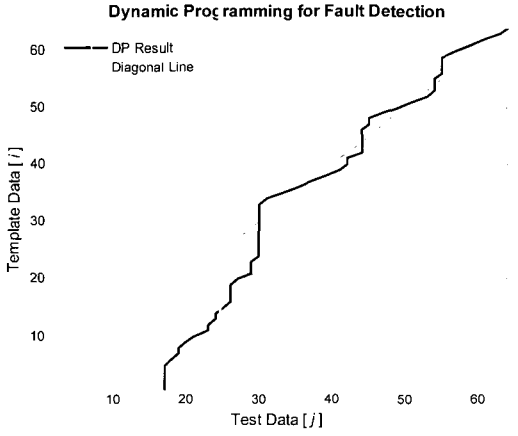

(b) Result of dynamic programming

Fig. 9. DTW result with two different data sets.

4.4 Results of fault identification

Four templates are calculated by 20 sets of 40 whole sets and the rest 20 sets are used for fault diagnosis. The templates are matched with fault signals by DTW and matching degrees are calculated.

As shown in Table 1, results for the bearing fault are sufficient to be used in the physical fields. Even though the difference signal of the bearing fault is similar with that of the misalignment, the identification ratio is 85% that means the bearing fault has the significant features for fault identification. The proposed method is suitable to detect and identify the broken rotor cases in this study.

As shown in Table 2, the correct identification ratio is 80% and it is possible to apply for fault diagnosis. The identification performance is not insufficient for physical application. The performance is the 2nd best in this study next to the result of the bearing fault that indicates the broken rotor has the significant feature for detection and diagnosis.

As shown in Table 3, the misalignment fault has indistinctive features with those of the bearing faults, therefore, it is difficult to diagnose. The identification ratio is 65% that is worse than that of the bearing fault. This indicates the patterns of the misalignment fault are not significantly extracted by the proposed method. This kind of the fault requires the other combined approach to improve the performance but it is not considered herein.

As shown in Table 4, the unbalance fault shows 70% of the identification ratio that is not so bad. This result means that the unbalance fault can be properly diagnosed by the proposed method. But there are some incorrect results of identification that have no significant pattern, so it is not easy to improve diagnosis performance. The broken rotor has the distinctive pattern, so the diagnosis performance can be improved by the other substitute algorithm. But the unbalance fault has no significant feature with other four faults, thus it is not easy to improve performance.

Table 1. Fault isolation results using bearing fault template

Fault type: Bearing Fault vs.			
Template: Bearing fault	Template: Broken rotor	Template: Misalignment	Template: Unbalance
7.596	12.127	14.975	10.321
7.223	31.381	9.930	10.888
7.421	25.030	7.841	11.863
6.305	34.179	9.478	9.995
7.244	40.214	14.799	11.346
10.013	33.812	11.836	14.327
6.188	27.659	7.635	9.443
9.792	52.513	23.640	13.380
10.492	39.859	10.713	17.279
8.709	43.289	21.056	13.363
9.483	47.126	18.798	12.996
22.751	28.822	6.023	27.498
13.780	32.576	8.812	13.974
12.762	21.571	8.939	19.085
5.583	8.157	21.441	11.699
11.771	36.577	16.160	17.657
6.776	33.762	10.763	11.621
4.960	54.953	24.083	11.998
20.696	40.022	21.285	21.940
13.263	31.873	15.749	19.403

Table 2. Fault isolation results using broken rotor template

Fault type: Broken Rotor vs.			
Template: Bearing fault	Template: Broken rotor	Template: Misalignment	Template: Unbalance
9.188	11.769	15.579	11.958
15.189	20.903	9.498	21.113
13.969	22.224	15.169	15.992
8.552	15.911	12.228	11.158
25.144	11.583	14.842	29.440
34.137	8.301	25.267	36.479
23.976	10.415	16.052	29.020
26.436	8.596	23.152	23.915
14.544	7.476	21.102	18.628
41.588	7.316	18.834	43.142
19.381	6.347	26.570	23.204
28.652	8.751	20.740	27.686
30.515	9.276	35.409	29.730
36.465	10.004	32.685	28.384
27.726	7.029	29.593	25.705
23.866	8.726	19.426	23.661
32.179	6.442	29.325	25.592
32.894	10.398	22.840	35.880
29.050	14.669	40.150	28.144
30.516	13.892	31.066	30.700

Table 3. Fault isolation results using misalignment template

Fault type: Misalignment vs.			
Template: Bearing fault	Template: Broken rotor	Template: Misalignment	Template: Unbalance
11.727	24.562	7.098	18.069
14.062	35.818	13.060	18.652
8.110	32.239	8.222	14.912
20.165	29.021	7.992	26.735
9.174	29.656	5.394	15.146
16.319	91.314	82.154	20.240
12.750	31.073	6.570	19.711
15.820	18.991	11.100	20.262
11.051	42.280	10.231	15.188
11.753	37.608	7.546	17.477
22.854	34.275	5.704	26.173
8.706	36.749	6.581	15.058
8.840	12.510	16.381	14.438
14.679	14.760	16.158	24.241
16.169	11.999	17.778	20.677
20.446	31.497	6.297	28.085
8.609	20.739	11.206	12.615
10.404	17.645	9.872	14.416
9.296	25.624	9.537	13.152
13.746	23.249	8.987	15.771

Table 4. Fault isolation results using unbalance template

Fault type: Unbalance vs.			
Template: Bearing fault	Template: Broken rotor	Template: Misalignment	Template: Unbalance
14.708	45.194	22.729	18.723
13.117	38.672	21.651	15.903
15.592	33.153	18.640	16.349
10.346	24.812	12.549	13.134
12.782	31.856	17.739	12.429
11.703	27.942	13.973	11.357
10.663	20.488	12.270	7.611
10.259	29.283	14.856	7.388
9.736	22.627	11.907	6.346
8.542	26.882	14.981	7.697
10.178	32.974	16.461	6.157
10.700	12.078	20.330	4.588
11.678	19.536	12.533	8.945
9.267	20.397	12.641	9.146
10.143	19.112	13.219	12.202
10.085	22.355	13.991	7.992
11.253	19.270	11.498	10.287
11.599	17.406	12.700	7.954
15.313	18.216	16.194	12.243
16.079	24.777	12.731	15.339

5. Conclusions

This paper described the time-series data mining that extracts features from time-series data such as supplied current signals of target motors. Wavelet transform applied in this study is the typical techniques for the time-series data mining.

The wavelet analysis method can detect most of the faults of induction motors. The bearing fault, broken rotor, misalignment, and unbalance fault were applied for fault detection and identification. The gradient and the 1st detail result of whole scales of wavelet decomposition were used.

For fault identification, instead of using classification models, the template matching method was applied to reduce computational load and easier analysis in fault diagnosis. The features of bearing fault and misalignment yield similar results in the wavelet analysis, so it shows worse identification results. In the future, the combined algorithm will be considered to improve performance of both faults.

References

[1] P. Vas, Parameter Estimation, Condition Monitoring, and Diagnosis of Electrical Machines, Clarendron Press, Oxford, 1993.

[2] G. B. Kliman and J. Stein, "Induction motor fault detection via passive current monitoring," International Conference in Electrical Machines, Cambridge, MA, pp.

13-17, August 1990.
[3] Y. E. Zhongming and W. U. Bin, "A Review on Induction Motor Online Fault Diagnosis," The Third International Power Electronics and Motion Control Conference (PIEMC 2000), vol. 3, pp. 1353-1358, Aug. 15-18, 2000.
[4] K. Abbaszadeh, J. Milimonfared, M. Haji, and H. A. Toliyat, "Broken Bar Detection in Induction Motor via Wavelet Transformation," IECON'01: The 27th Annual Conference of the IEEE Industrial Electronics Society, pp. 95-99, 2001.
[5] M. Haji and H. A. Toliyat, "Pattern Recognition-A Technique for Induction Machines Rotor Fault Detection Eccentricity and Broken Bar Fault," Conference Record of the 2001 IEEE Industry Applications Conference, vol. 3, pp. 1572-1578, 30 Sept.-4 Oct. 2001.
[6] S. Nandi, H. A. Toliyat, "Condition Monitoring and Fault Diagnosis of Electrical Machines - A Review," IEEE Industry Applications Conference, vol. 1, pp. 197-204, 1999.
[7] B. Yazici, G. B. Kliman, "An Adaptive Statistical Time-Frequency Method for Detection of Broken Bars and Bearing Faults in Motors Using Stator Current," IEEE Trans. on Industry Application, vol. 35, no. 2, pp. 442-452, March/April 1999.
[8] S. Mallat, A Wavelet Tour of Signal Processing. San Diego, CA: Academic, 1998.
[9] I. Daubechies, Ten Lectures on Wavelets. Philadelphia, PA: SIAM, 1992.
[10] Y. Meyer, Wavelets: Algorithms and Applications. Philadelphia, PA: SIAM, 1993.
[11] H. Sakoe and S. Chiba, "Dynamic Programming Algorithm Optimization for Spoken Word Recognition," IEEE trans. on Acoustics, Speech and Signal Processing, vol. 26, no. 1, pp. 43-49, February 1978.
[12] H. Sakoe, R. Isotani, K. Yoshida, K. Iso, and T. Watanabe, "Speaker-Independent Word Recognition Using Dynamic Programming Neural Networks," Proc. Of The IEEE Int. Conf. On Acoustics, Speech and Signal Processing, ICASSP '89, pp. 29-32, 1989.

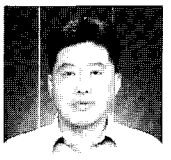

Hyeon Bae
He received the M.S. and Ph.D. degree in electrical engineering from Pusan National University in 2001 and 2005, respectively. His research interests include intelligent system and control, data mining, systems bilogy, and bioinformatics.

Sungshin Kim
He received the B.S. and M.S. degrees from Yonsei University, and the Ph.D. degree in electrical engineering from Georgia Institute of Technology, Atlanta, in 1984, 1986, and 1996, respectively. He is currently an Associate Professor in the School of Electrical and Computer Engineering, Pusan National University. His research interests include intelligent control, fuzzy logic control, manufacturing systems, and data mining.

George J. Vachtsevanos
He attended the City College of New York and received his B.E.E. degree in 1962. He received an M.E.E. degree from New York University and his Ph.D. degree in Electrical Engineering from the City University of New York in 1970. His research focused on adaptive control systems. Since joining the faculty at Georgia Tech, he has been teaching courses and conducting research on intelligent systems, robotics and automation of industrial processes and diagnostics/prognostics of large-scale complex systems.